

Hydrogen bonding *versus* $lp-\pi$ and $\pi-\pi$ interactions: their key competition in sildenafil solvates

Rafael Barbas,^a Rafel Prohens,^{*,a} Mercè Font-Bardia,^b Antonio Bauzá,^c and Antonio Frontera^{*,c}

^aUnitat de Polimorfisme i Calorimetria, Centres Científics i Tecnològics, Universitat de Barcelona, Baldiri Reixac 10, 08028 Barcelona, Spain. E-mail: rafel@ccit.ub.edu.

^bUnitat de Difracció de Raigs X, Centres Científics i Tecnològics, Universitat de Barcelona.

^cDepartament de Química, Universitat de les Illes Balears, Crta. de Valldemossa km 7.5, 07122 Palma (Balears), Spain. E-mail: toni.frontera@uib.es.

Electronic Supplementary Information

Table of contents:

1. Theoretical methods	2
2. Figure S1	2
3. Figures S2 and S3.....	3
4. Table S1	4
5. Experimental methods	5
6. Crystal data and structure refinement	7
7. Characterization of the solids	11
8. References.....	18

1. Theoretical methods

The energies of all complexes included in this study were computed at the M06-2X/def2-TZVP level of theory. We have used the crystallographic coordinates for the theoretical analysis of the noncovalent interactions present in the solid state. For the calculations regarding the open and closed conformations of sildenafil we have used the BP86-D3/def2-TZVP level of theory, which includes the latest available correction for dispersion (D3).ⁱ The calculations have been performed by using the program TURBOMOLE version 7.0.ⁱⁱ The interaction energies were calculated with correction for the basis set superposition error (BSSE) by using the Boys–Bernardi counterpoise technique.ⁱⁱⁱ The MEPS calculations have been performed by means of the SPARTAN software.^{iv} The NCI plot is a visualization index based on the electron density and its derivatives, and enables identification and visualization of non-covalent interactions efficiently. The isosurfaces correspond to both favorable and unfavorable interactions, as differentiated by the sign of the second density Hessian eigenvalue and defined by the isosurface color. NCI analysis allows an assessment of host-guest complementarity and the extent to which weak interactions stabilize a complex. The information provided by NCI plots is essentially qualitative, i.e. which molecular regions interact. The color scheme is a red-yellow-green-blue scale with red for ρ^+_{cut} (repulsive) and blue for ρ^-_{cut} (attractive). Yellow and green surfaces correspond to weak repulsive and weak attractive interactions, respectively.^v

2. Figure S1

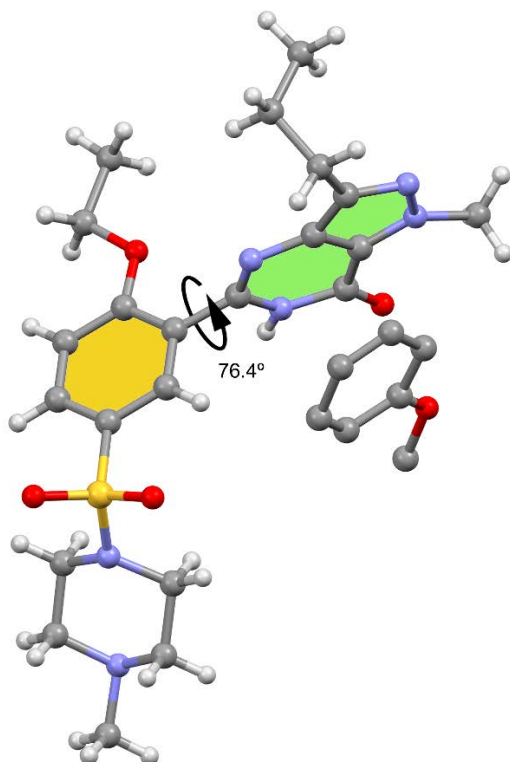


Fig. S1 X-ray structure of compound **3** with indication of the rotational angle

3. Figure S2

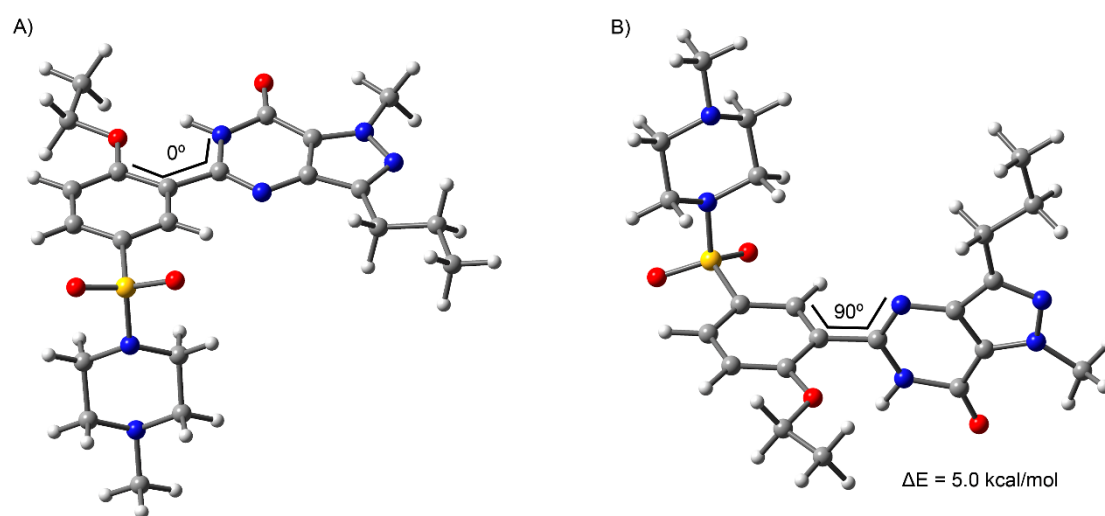


Fig. S2 Optimized open (A) and closed (B) conformations of sildenafil at the BP86-D3/def2-TZVP level of theory

3. Figure S3

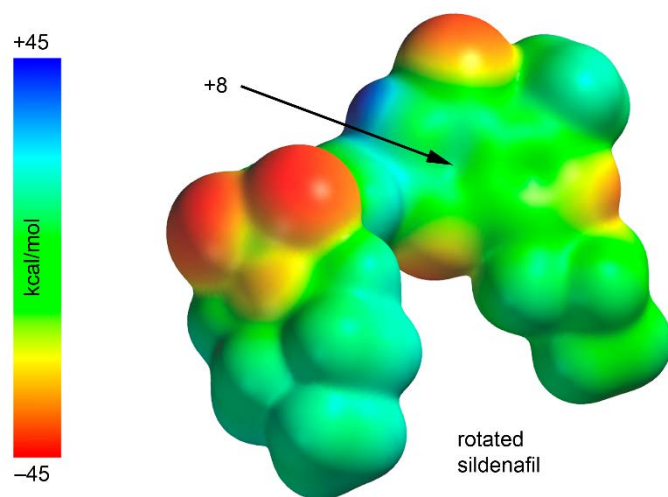


Fig. S3. MEP surface of sildenafil rotated 90 degrees.

4. Table S1. CCSD codes of sildenafil salts and/or solvates

Database Identifier	Deposition Number	salt/solvate	DOI
FEDTEO	264096	citrate monohydrate	10.1107/S1600536805002564
KAJYIG	1062242	Citrate hemihydrate	10.1039/C5CE02234G
QEGTUT	853915	none	10.5560/ZNB.2012-0073
QEKVEI	600018	saccharinate hemikis(ethanol)	10.1021/cg0601150
QEKVIM	600019	saccharinate ethanol	10.1021/cg0601150
QEKVOS	600020	saccharinate	10.1021/cg0601150
QEKVUY	600021	hemikis(dimethylsulfoxide) saccharinate nitromethane	10.1021/cg0601150
QEKWAF	600025	saccharinate hemikis(pyrrolidinone)	10.1021/cg0601150
QEKWEJ	600026	saccharinate	10.1021/cg0601150
QEKWIN	600027	saccharinate formamide	10.1021/cg0601150
QEKWOT	600028	saccharinate hemikis(1,4- dioxane)	10.1021/cg0601150
QEKWUZ	600029	saccharinate hemikis(ethylene glycol)	10.1021/cg0601150
QEMLEA	600022	saccharinate hemikis(dimethylformamide)	10.1021/cg0601150
QEMLIE	600023	saccharinate acetonitrile	10.1021/cg0601150
QEMLOK	600024	saccharinate dihydrate	10.1021/cg0601150
WOYHAV	990216	salicylate	10.1016/j.mencom.2015.01.018
YAJHEZ	1484239	thiosaccharinate	10.1021/acs.cgd.6b01669
YIWWIM	956673	hemikis(oxalate)	10.1021/mp400516b
YIWWOS	956674	hydrogenfumarate trihydrate	10.1021/mp400516b
YIWWUY	956675	hemikis(succinate) monohydrate	10.1021/mp400516b
YIWXAF	956676	hemikis(glutarate)	10.1021/mp400516b
YIWXEJ	956677	adipic acid solvate	10.1021/mp400516b
YIWXIN	956678	pimelic acid solvate	10.1021/mp400516b
YIWXOT	956679	suberic acid solvate	10.1021/mp400516b

5. Experimental methods

5.1. Materials and measurements.

Sildenafil used was of reagent grade and used as received from Polpharma (form I). Chloroform solvate (solvate 1) has been obtained by slow crystallization in chloroform after 5 days at 25 °C. Toluene solvate (solvate 2) has been obtained by crystallization in toluene after 1 day at 25 °C. Anisole solvate (solvate 3) has been obtained by slow crystallization in anisole after 25 days at 25 °C. Dioxane solvate (solvate 4) has been obtained by slow crystallization in a mixture dioxane-acn (equimolar ratio) after 21 days at 25 °C

5.2. X-ray crystallographic analysis.

Single crystal X-ray diffraction intensity data of Sildenafil form I and acetonitrile solvate form I were collected using a D8 Venture system equipped with a multilayer monochromator and a Mo microfocus ($\lambda = 0.71073 \text{ \AA}$). Frames were integrated with the Bruker SAINT software package using a SAINT algorithm. Data were corrected for absorption effects using the multi-scan method (SADABS).^{vi} The structure was solved and refined using the Bruker SHELXTL Software Package, a computer program for automatic solution of crystal structures and refined by full-matrix least-squares method with ShelXle Version 4.8.0, a Qt graphical user interface for SHELXL computer program.^{vii} Powder X-ray diffraction patterns of form II were obtained on a PANalytical X'Pert PRO MPD diffractometer in transmission configuration using Cu K α 1+2 radiation ($\lambda = 1.5406 \text{ \AA}$) with a

focalizing elliptic mirror and a PIXcel detector working at a maximum detector's active length of 3.347° . Configuration of convergent beam with a focalizing mirror and a transmission geometry with flat samples sandwiched between low absorbing films measuring from 2 to 40° in 2θ , with a step size of 0.026° and a total measuring time of 30 minutes.

5.3 Differential Scanning Calorimetry (DSC). Differential scanning calorimetry analysis were carried out by means of a Mettler-Toledo DSC-822e calorimeter. Experimental conditions: aluminium crucibles of $40\ \mu\text{L}$ volume, atmosphere of dry nitrogen with $50\ \text{mL}/\text{min}$ flow rate, heating rate of $10^\circ\text{C}/\text{min}$. The calorimeter was calibrated with indium of 99.99% purity.

5.4 Thermogravimetric Analysis (TGA). Thermogravimetric analyses were performed on a Mettler-Toledo TGA-851e thermobalance. Experimental conditions: alumina crucibles of $70\ \mu\text{L}$ volume, atmosphere of dry nitrogen with $50\ \text{mL}/\text{min}$ flow rate, heating rate of $10^\circ\text{C}/\text{min}$.

5.5 List of solvents used in the solid forms screening. Methanol, ethanol, IPA, butanol, 1-propanediol, glycerol, ethylene glycol, 2-methoxyethanol, 1-propanol, 1-pentanol, 1-octanol, 2,2,2-trifluoroethanol, benzyl alcohol, ACN, propionitrile, MEK, acetone, MiBK, water, DMF, DMSO, pentane, heptane, cyclohexane, hexane, methylcyclohexane, toluene, xylene, mesitylene, anisole, 2-nitrotoluene, nitrobenzene, AcOEt, isopropyl acetate, diethylether, THF, 1-methyl-2-pyrrolidone, dimethyl ethylene glycol, diisopropyl ether, dioxane, iodomethane, dichloromethane, 1,2-dichloroethane, chloroform, 1,1,1-trichloroethane, 1,1,2-trichloroethane, formic acid, acetic acid, trifluoroacetic acid, propanoic acid, NH_3 (32%) in water, diethylamine, trimethylamine and pyridine.

6.- Crystal data and structure refinement

6.1 Chloroform solvate (solvate 1) (mo_023WB13A_0ma_a)

Table S2. Crystal data and structure refinement for mo_023WB13A_0ma_a.

Identification code	mo_023WB13A_0ma_a	
Empirical formula	C ₂₃ H ₃₁ Cl ₃ N ₆ O ₄ S	
Formula weight	593.95	
Temperature	301(2) K	
Wavelength	0.71073 Å	
Crystal system	Orthorhombic	
Space group	P b c a	
Unit cell dimensions	a = 16.3399(7) Å	α = 90°.
	b = 8.5767(3) Å	β = 90°.
	c = 40.1148(16) Å	γ = 90°.
Volume	5621.8(4) Å ³	
Z	8	
Density (calculated)	1.403 Mg/m ³	
Absorption coefficient	0.441 mm ⁻¹	
F(000)	2480	
Crystal size	0.303 x 0.184 x 0.124 mm ³	
Theta range for data collection	2.383 to 26.466°.	
Index ranges	-20 ≤ h ≤ 17, -10 ≤ k ≤ 10, -46 ≤ l ≤ 50	
Reflections collected	35024	
Independent reflections	5787 [R(int) = 0.0421]	
Completeness to theta = 25.242°	99.8 %	
Absorption correction	Semi-empirical from equivalents	
Max. and min. transmission	0.7454 and 0.6894	
Refinement method	Full-matrix least-squares on F ²	

Data / restraints / parameters	5787 / 0 / 338
Goodness-of-fit on F^2	1.026
Final R indices [$I > 2\sigma(I)$]	R1 = 0.0661, wR2 = 0.1718
R indices (all data)	R1 = 0.1117, wR2 = 0.1981
Extinction coefficient	n/a
Largest diff. peak and hole	0.678 and -0.634 e. \AA^{-3}

6.2 Toluene solvate (solvate 2) (mo_023UB111_0ma_aa)

Table S3. Crystal data and structure refinement for mo_023UB111_0ma_aa.

Identification code	mo_023ub111_0ma_aa	
Empirical formula	C ₅₁ H ₆₈ N ₁₂ O ₈ S ₂	
Formula weight	1041.29	
Temperature	100(2) K	
Wavelength	0.71073 Å	
Crystal system	Monoclinic	
Space group	P 21/c	
Unit cell dimensions	a = 14.8287(6) Å	α = 90°.
	b = 14.3781(6) Å	β = 106.4830(10)°.
	c = 12.7277(5) Å	γ = 90°.
Volume	2602.13(18) Å ³	
Z	2	
Density (calculated)	1.329 Mg/m ³	
Absorption coefficient	0.169 mm ⁻¹	
F(000)	1108	
Crystal size	0.666 x 0.106 x 0.092 mm ³	
Theta range for data collection	2.189 to 28.728°.	
Index ranges	-18 ≤ h ≤ 20, -19 ≤ k ≤ 19, -17 ≤ l ≤ 16	
Reflections collected	59166	
Independent reflections	6727 [R(int) = 0.0416]	
Completeness to theta = 25.242°	99.7 %	
Absorption correction	Semi-empirical from equivalents	
Max. and min. transmission	0.7458 and 0.6943	
Refinement method	Full-matrix least-squares on F ²	
Data / restraints / parameters	6727 / 0 / 322	
Goodness-of-fit on F ²	1.044	
Final R indices [I > 2σ(I)]	R1 = 0.0339, wR2 = 0.0949	
R indices (all data)	R1 = 0.0415, wR2 = 0.09941	
Extinction coefficient	n/a	
Largest diff. peak and hole	1.364 and -1.000 e.Å ⁻³	

6.3 Anisole solvate (solvate 3) (mo_023UB122_0ma_aa)

Table S4. Crystal data and structure refinement for mo_023UB122_0ma_aa.

Identification code	mo_023ub122_0ma_aa	
Empirical formula	C51 H68 N12 O9 S2	
Formula weight	1057.29	
Temperature	100(2) K	
Wavelength	0.71073 Å	
Crystal system	Monoclinic	
Space group	P 21/c	
Unit cell dimensions	a = 14.8822(7) Å	$\alpha = 90^\circ$.
	b = 14.2697(7) Å	$\beta = 106.409(2)^\circ$.
	c = 12.8142(6) Å	$\gamma = 90^\circ$.
Volume	2610.4(2) Å ³	
Z	2	
Density (calculated)	1.345 Mg/m ³	
Absorption coefficient	0.170 mm ⁻¹	
F(000)	1124	
Crystal size	0.435 x 0.116 x 0.096 mm ³	
Theta range for data collection	2.018 to 30.560°.	
Index ranges	-21 ≤ h ≤ 21, -20 ≤ k ≤ 20, -16 ≤ l ≤ 18	
Reflections collected	95257	
Independent reflections	8010 [R(int) = 0.0385]	
Completeness to theta = 25.242°	99.9 %	
Absorption correction	Semi-empirical from equivalents	
Max. and min. transmission	0.7461 and 0.7218	
Refinement method	Full-matrix least-squares on F ²	
Data / restraints / parameters	8010 / 0 / 323	
Goodness-of-fit on F ²	1.037	
Final R indices [I > 2σ(I)]	R1 = 0.0585, wR2 = 0.1644	
R indices (all data)	R1 = 0.0658, wR2 = 0.1704	
Extinction coefficient	n/a	
Largest diff. peak and hole	2.299 and -2.520 e.Å ⁻³	

6.4 Dioxane solvate (solvate 4) (mo_023WB33_0ma_a)

Table S5. Crystal data and structure refinement for mo_023WB33_0ma_a.

Identification code	mo_023WB33_0ma_a	
Empirical formula	C ₂₄ H ₃₄ N ₆ O ₅ S	
Formula weight	518.63	
Temperature	100(2) K	
Wavelength	0.71073 Å	
Crystal system	Monoclinic	
Space group	P 21/c	
Unit cell dimensions	a = 15.6055(5) Å	α = 90°.
	b = 13.5523(4) Å	β = 106.3620(10)°.
	c = 12.5064(4) Å	γ = 90°.
Volume	2537.86(14) Å ³	
Z	4	
Density (calculated)	1.357 Mg/m ³	
Absorption coefficient	0.175 mm ⁻¹	
F(000)	1104	
Crystal size	0.227 x 0.057 x 0.039 mm ³	
Theta range for data collection	2.267 to 26.780°.	
Index ranges	-19 ≤ h ≤ 19, -17 ≤ k ≤ 17, -14 ≤ l ≤ 15	
Reflections collected	27836	
Independent reflections	5382 [R(int) = 0.0542]	
Completeness to theta = 25.242°	99.4 %	
Absorption correction	Semi-empirical from equivalents	
Max. and min. transmission	0.7454 and 0.6929	
Refinement method	Full-matrix least-squares on F ²	
Data / restraints / parameters	5382 / 0 / 333	
Goodness-of-fit on F ²	0.999	
Final R indices [I > 2σ(I)]	R1 = 0.0405, wR2 = 0.0955	
R indices (all data)	R1 = 0.0661, wR2 = 0.1181	
Extinction coefficient	n/a	
Largest diff. peak and hole	0.318 and -0.489 e.Å ⁻³	

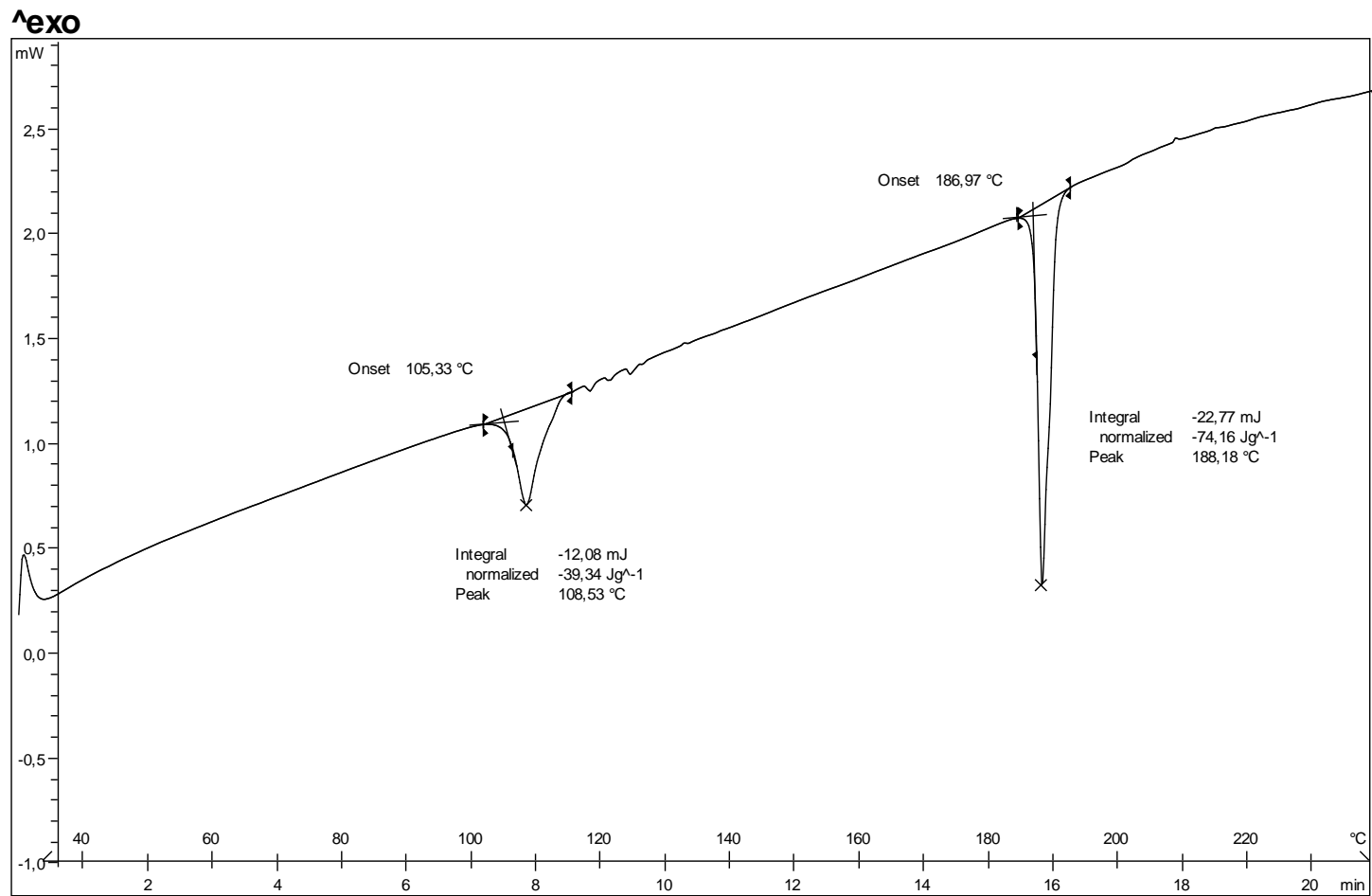
Table S6. NH...N Hydrogen bonds for solvates **2-4** [Å and °].

Solvate	d(D-H)	d(H...A)	d(D...A)	<(DHA)
2(i)	0.95(2)	1.95(2)	2.889(1)	174(2)
3(i)	0.88	2.06	2.934(2)	177
4(ii)	0.94(3)	1.95(3)	2.892(2)	176(2)

⁽ⁱ⁾[x,3/2-y,1/2+z] ; ⁽ⁱⁱ⁾ [x,1/2-y,1/2+z]

7.- Characterization of the solids

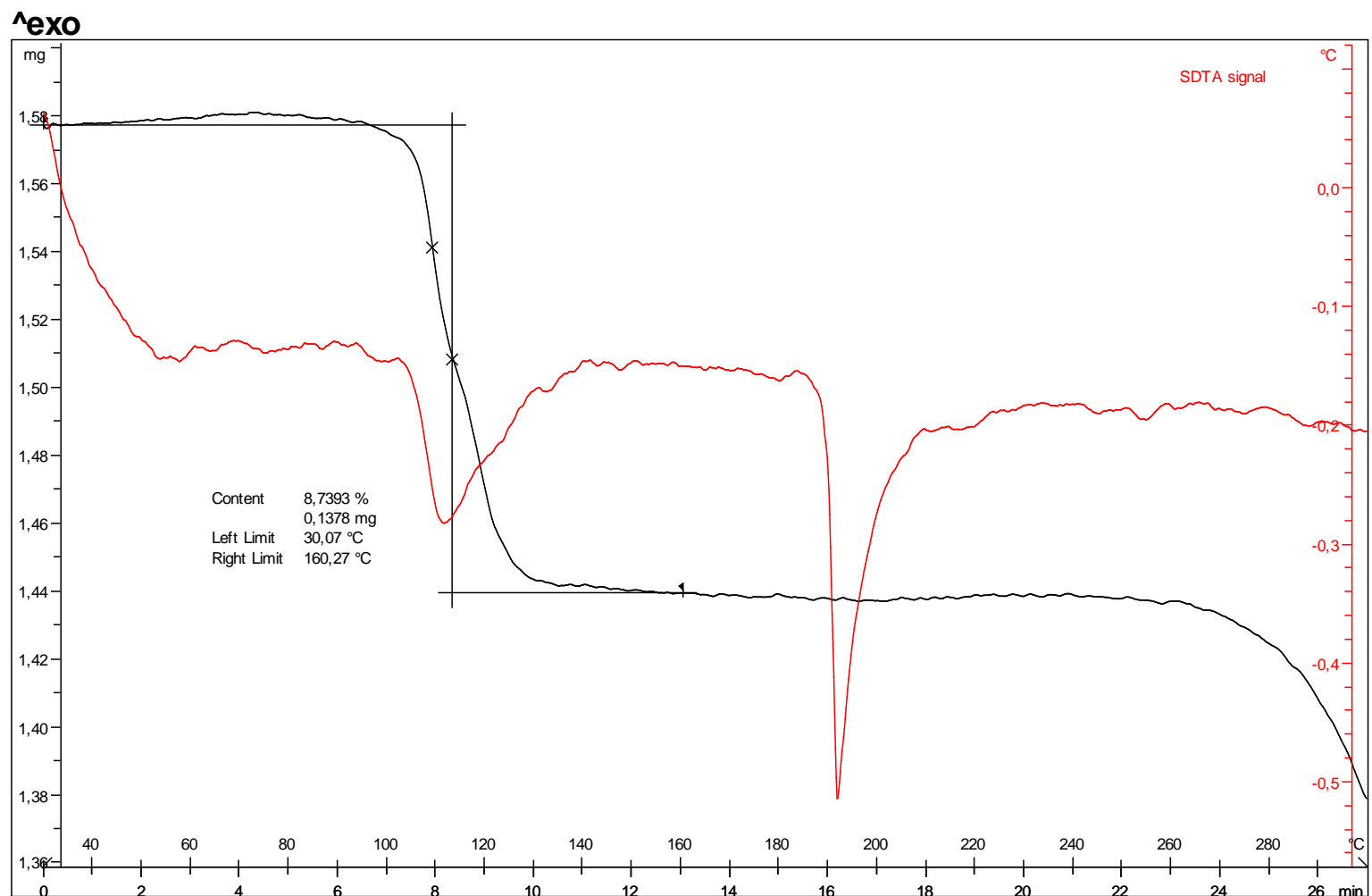
Figure S3: DSC of solvate 2 at 10 °C/min (toluene solvate)



Unitat de Polimorfisme i Calorimetria: CPV

STAR[®] SW 8.10

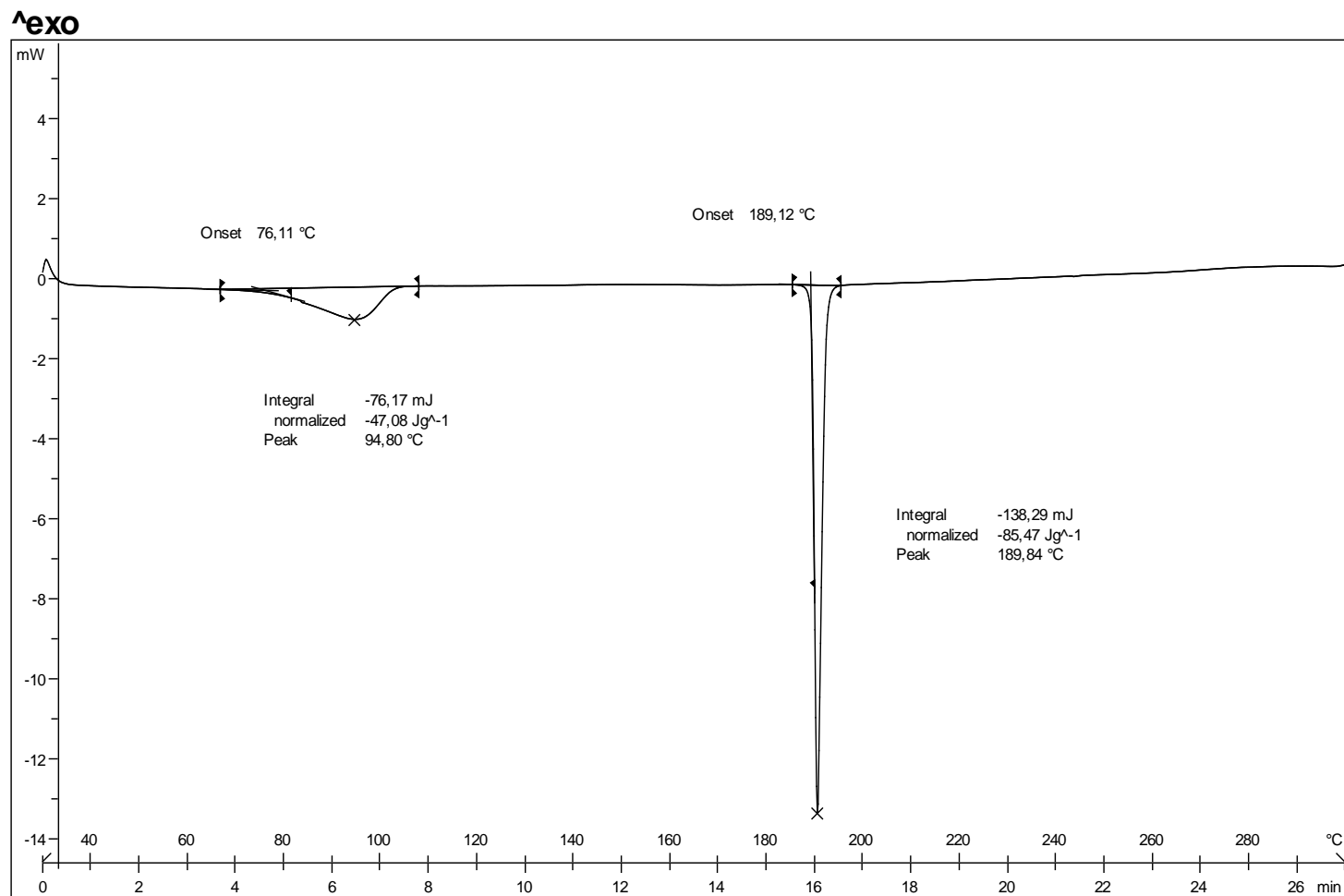
Figure S4: TGA of solvate 2 at 10 °C/min (toluene solvate)



Unitat de Polimorfisme i Calorimetria: CPV

STAR^e SW 8.10

Figure S5: DSC of solvate 3 at 10 °C/min (anisole solvate)



Unitat de Polimorfisme i Calorimetria: CPV

STAR^e SW 8.10

Figure S6: TGA of solvate 3 at 10 °C/min (anisole solvate)

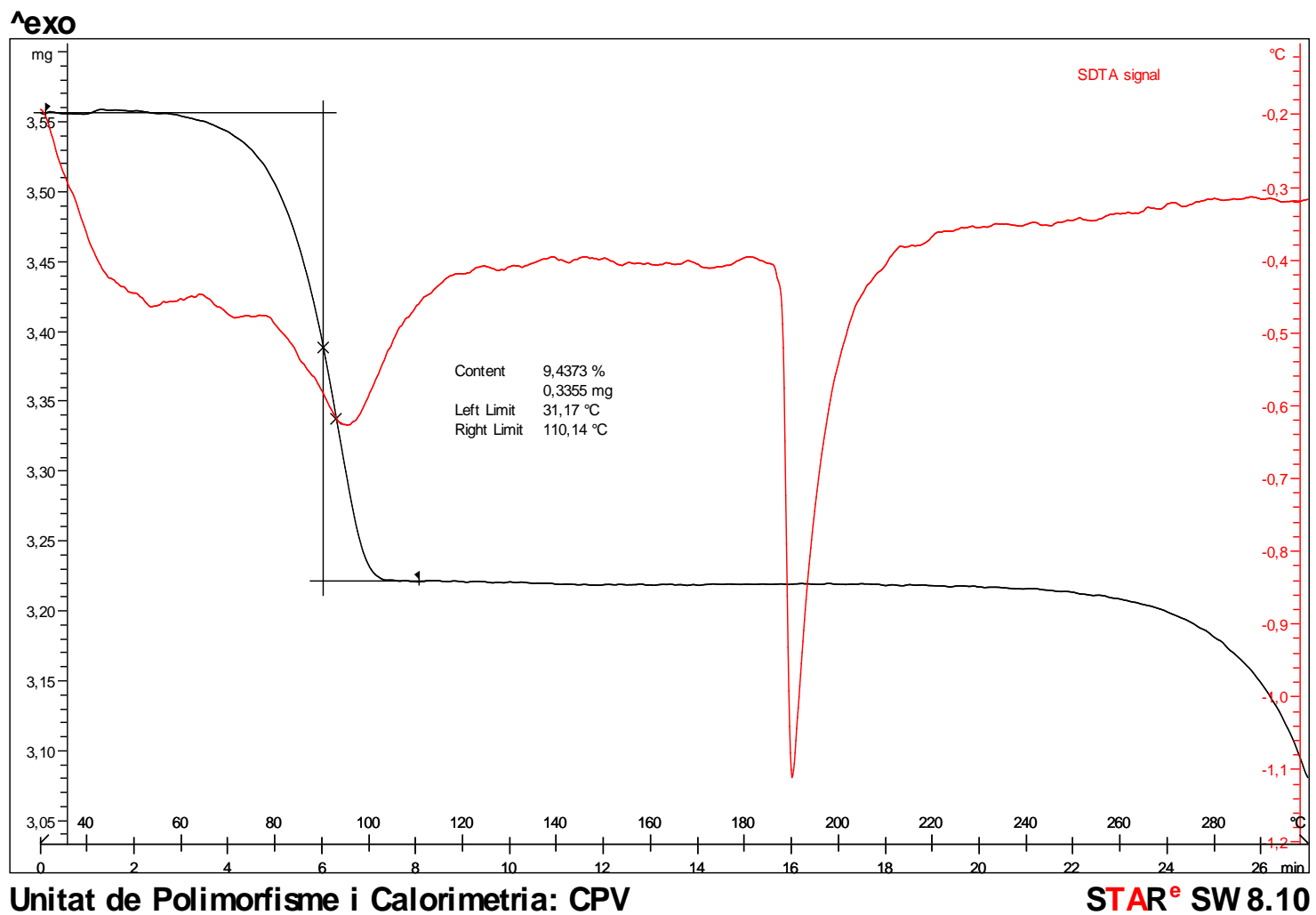
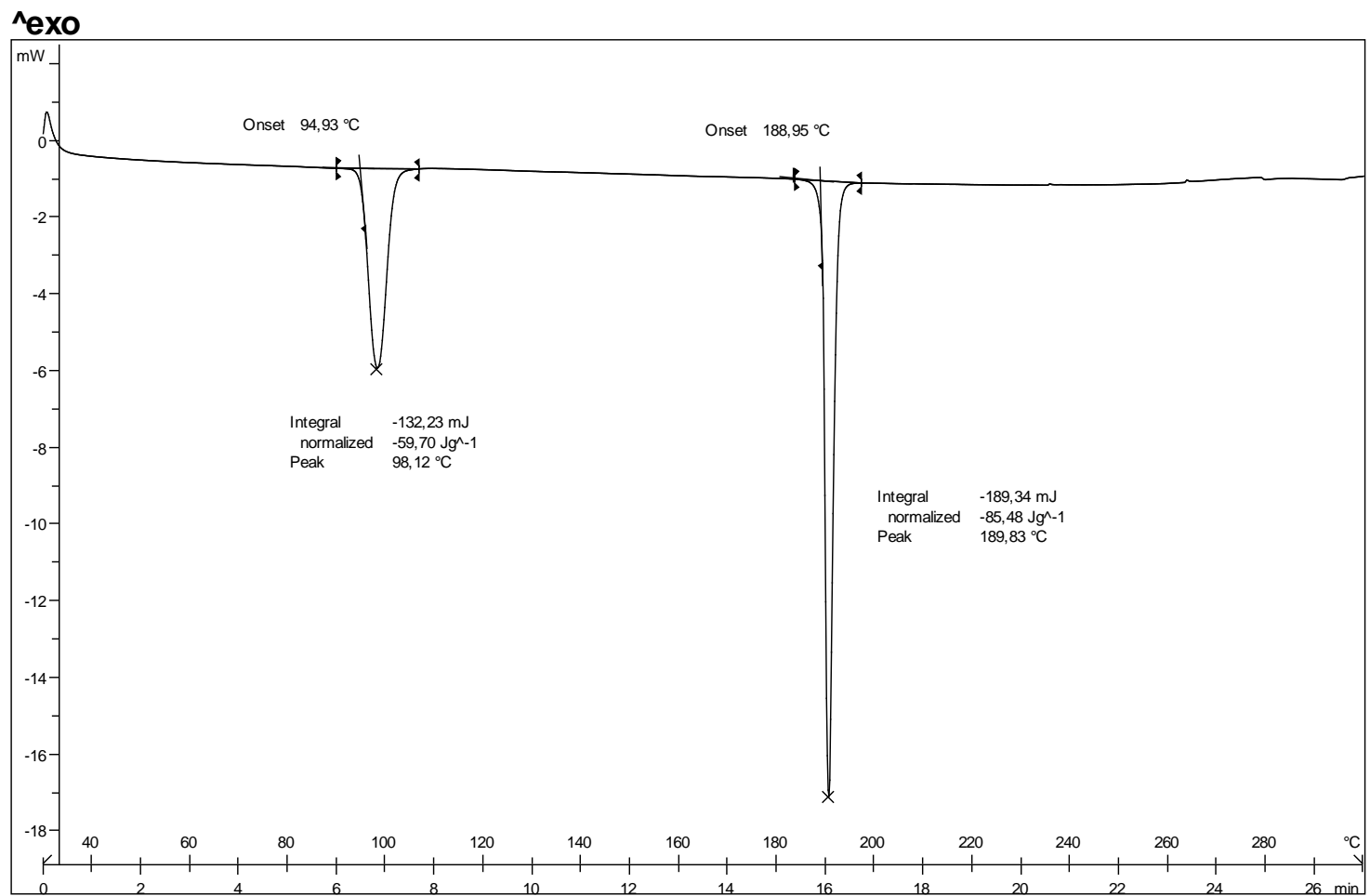


Figure S7: DSC of solvate 4 at 10 °C/min (dioxane solvate)



Unitat de Polimorfisme i Calorimetria: CPV

STAR^e SW 8.10

Figure S8: TGA of solvate 4 at 10 °C/min (dioxane solvate)

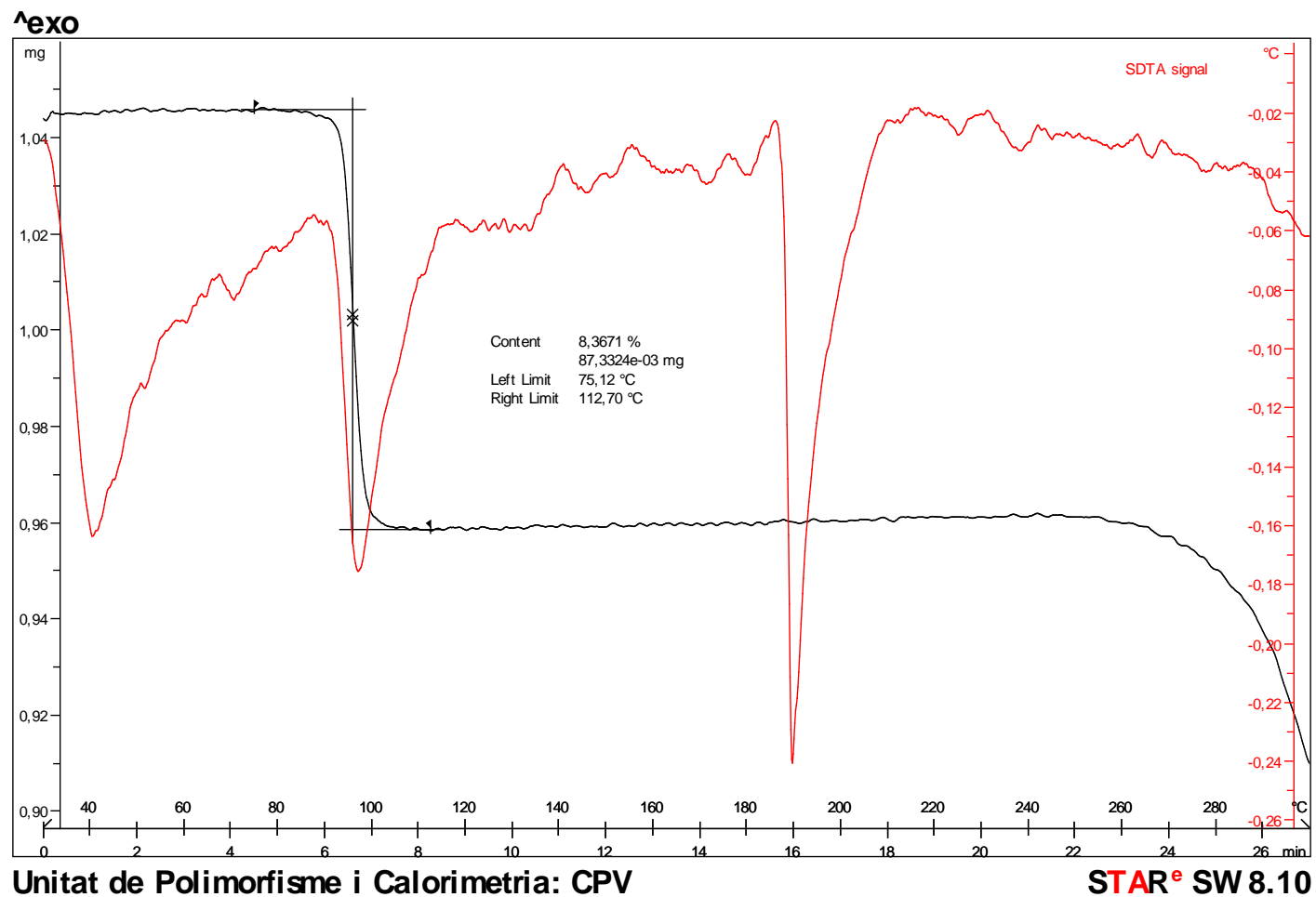
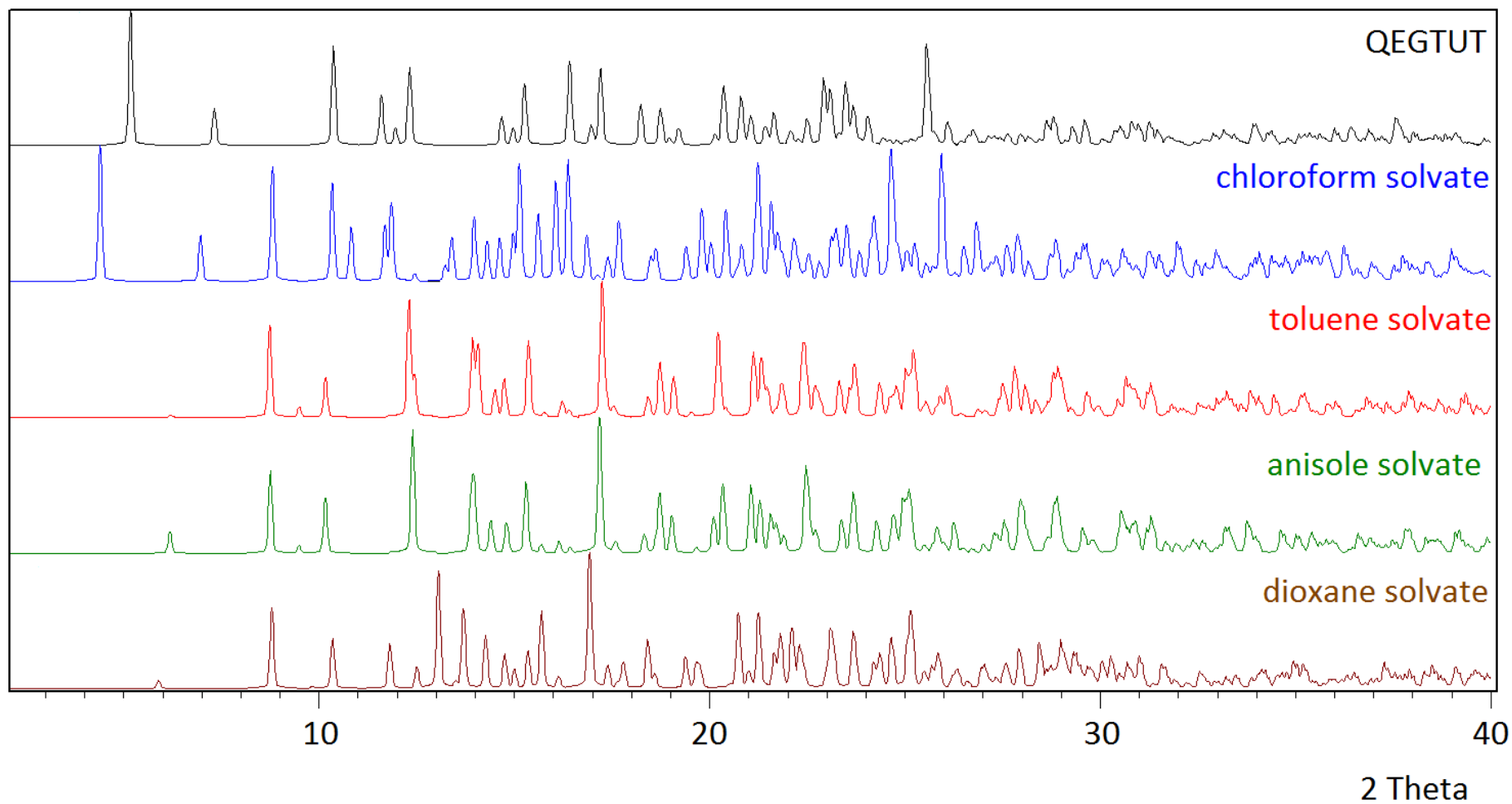


Figure S9: Comparison of the simulated PXRD of different solvates from 2 to 40 2θ



8.- References

- ⁱ S. Grimme, J. Antony, S. Ehrlich, and H. Krieg, *J. Chem. Phys.*, 2010, **132**, 154104–19.
- ⁱⁱ R. Ahlrichs, M. Bär, M. Hacer, H. Horn and C. Kömel, *Chem. Phys. Lett.*, 1989, **162**, 165–169.
- ⁱⁱⁱ S. B. Boys and F. Bernardi, *Mol. Phys.*, 1970, **19**, 553–566.
- ^{iv} Y. Shao, L.F. Molnar, Y. Jung, J. Kussmann, C. Ochsenfeld, S.T. Brown, A.T.B. Gilbert, L.V. Slipchenko, S.V. Levchenko, D.P. O’Neill, R.A. DiStasio Jr., R.C. Lochan, T. Wang, G.J.O. Beran, N.A. Besley, J.M. Herbert, C.Y. Lin, T. Van Voorhis, S.H. Chien, A. Sodt, R.P. Steele, V.A. Rassolov, P.E. Maslen, P.P. Korambath, R.D. Adamson, B. Austin, J. Baker, E.F.C. Byrd, H. Dachsel, R.J. Doerksen, A. Dreuw, B.D. Dunietz, A.D. Dutoi, T.R. Furlani, S.R. Gwaltney, A. Heyden, S. Hirata, C-P. Hsu, G. Kedziora, R.Z. Khalliulin, P. Klunzinger, A.M. Lee, M.S. Lee, W.Z. Liang, I. Lotan, N. Nair, B. Peters, E.I. Proynov, P.A. Pieniazek, Y.M. Rhee, J. Ritchie, E. Rosta, C.D. Sherrill, A.C. Simmonett, J.E. Subotnik, H.L. Woodcock III, W. Zhang, A.T. Bell, A.K. Chakraborty, D.M. Chipman, F.J. Keil, A. Warshel, W.J. Hehre, H.F. Schaefer, J. Kong, A.I. Krylov, P.M.W. Gill and M. Head-Gordon, *Phys. Chem. Chem. Phys.*, 2006, **8**, 3172–3191.
- ^v J. Contreras-García, E. R. Johnson, S. Keinan, R. Chaudret, J-P.Piquemal, D. N. Beratan and W. Yang *J. Chem. Theory and Comput.*, 2011, **7**, 625–632.
- ^{vi} SADABS Bruker AXS; Madison, Wisconsin, USA, 2004; SAINT, Software Users Guide, Version 6.0; Bruker Analytical X-ray Systems, Madison, WI, 1999. Sheldrick, G. M. SADABS v2.03: Area–Detector Absorption Correction. University of Göttingen, Germany, 1999; Saint Version 7.60A (Bruker AXS 2008); SADABS V. 2008–1 (2008).
- ^{vii} Sheldrick, G. M. *Acta Cryst.* 2008, **A64**, 112–122.